



ADSORPTION STUDIES OF ZINC(II) IONS ON BIOPOLYMER COMPOSITE BEADS OF ALGINATE-FLY ASH

Uzma Nadeem^[a] and Monika Datta^{[a]*}

Keywords: biopolymer beads; sodium alginate; adsorption; isotherm models; wastewater

The gelling and metal-chelating properties of alginate were combined to develop an adsorbent for heavy metal removal. Biopolymer beads composed of fly ash and sodium alginate proved to be an effective adsorbent for removal of Zn(II) ions from aqueous solutions. The effect of initial pH (2–10), bead dose (10–80), agitation time (1–24 h), beads composition (0.1 g–0.7 g fly ash) and Zn(II) ions initial concentration (5–30 mg L⁻¹) on the adsorption process, as well as to what extent the adsorption data obey Langmuir and Freundlich adsorption isotherms were investigated. The maximum adsorption was found 84.20 % within 8 h and after that reaches equilibrium. The adsorption of Zn(II) ions is quite sensitive to pH of the suspension and shows an optimum uptake value at pH 6.0. Maximum adsorption occurred for 40 beads and in case of composition, beads composed of 0.5 g fly ash has shown good results. It is clear from the experimental results that the pH plays an important role in adsorption of zinc ions. The average size, bulk density and swelling ratio of beads calculated are; 0.12 cm, 0.34 g mL⁻¹ and 28.65 respectively. The synthesized beads were also characterized by FTIR, XRD, SEM, TGA/DTA and other methods.

*Corresponding Authors

E-Mail: monikadatta_chem@yahoo.co.in

[a] Department of Chemistry, University of Delhi, Delhi, 110007, India.

[a] E-Mail: uzmanadeem3@gmail.com

Department of Chemistry, University of Delhi, Delhi, 110007, India.

Introduction

Environmental pollution by heavy metals which are released into the environment through various anthropogenic activities such as mining, energy and fuel production¹, electroplating, wastewater sludge treatment and agriculture are one of the world's major environmental problems. This is probably due to rapid industrialization^{2,3}, population growth and complete disregard for the environmental health. Initially, heavy metals are naturally present in soils as natural components but as of now, the presence of heavy metals in the environment has accelerated due to human activities. Even though zinc is an essential requirement for a healthy body⁴, excess zinc can be harmful, and cause zinc toxicity.⁵⁻⁸ The free zinc ions in solution is highly toxic to plants, invertebrates, and even vertebrate fish. Stomach acid contains hydrochloric acid, in which metallic zinc dissolves readily to give corrosive zinc chloride, which can cause damage to the stomach lining due to the high solubility of the zinc ion in the acidic stomach.

Fly ash is a significant waste that is released of thermal power plants and defined as very fine particles that are drifted upward with up taken by the flue gases due to the burning of used coal.⁹ Fly ash, a finely divided and powdered by-product, from coal fired power plants or biomass combustion facilities requires ultimate disposal. Studies on the country and the world of fly ash usage has increased in the last two decades and as a result of these studies have been identified fly ash as a suitable adsorbent for the adsorption of heavy metals from waste water.¹⁰ The major constituents of fly ash are silica, alumina, and iron

oxide, which are ideal metal adsorbents. In recent years, fly ash has been employed as a low-cost adsorbent for gas and water cleaning¹¹ and much effort have been focused on heavy metal and dye adsorption on fly ash particles.¹²

Recently numerous approaches have been studied for the development of cheaper and more effective adsorbents containing natural polymers. The use of naturally occurring biopolymer seems to be a preferred alternative to the use of expensive chemical adsorbents for the removal of heavy metal ions. Adsorption onto polysaccharide derivatives can be a low-cost procedure of choice in water decontamination. Among the industrially attractive polysaccharide biopolymers, alginate is known to have high complex formation ability with various heavy metals.¹³

Sodium alginate was chosen as the material for preparation of the carrier matrix because it is a natural, biodegradable, biocompatible, non toxic orally and hydrophilic polymer suitable for the entrapment of water soluble toxicants. They produce thermally irreversible gels by association with most divalent cations. Alginates are polysaccharides found in brown seaweeds and are composed mainly of linear polymers of β -(1 \rightarrow 4)-D-mannuronic (M) and α -L-guluronic (G) acids differing in terms of their proportions and linear arrangements. Different species of algae contain different percentages of mannuronic acid (M) and guluronic acid (G). Because of the differences in conformation of the two different residues, gelation with divalent cations can be attributed mainly to the G residue (especially to the pure polyguluronic (GG) chains), while the M residue contributes mainly to the cation exchange capacity of this naturally occurring polymer. Hydroxyl groups have been found to play an important role not only in cation exchange capacity but also in the affinity of the material towards different metal ions.¹⁴

The mechanisms of biosorption are not fully understood, but it is well known that alginates of algal cell walls play an important role in metal binding.¹⁵

In the present work the gelling and metal-chelating properties of alginate were combined with fly ash to develop composite adsorbents for heavy metal removal.

Experimental

Reagents

Sodium alginate was obtained from Thomas Baker Pvt. Limited. The fly ash obtained from National Thermal Power Corporation was grounded and sieved to a particle size of 200–400 micron. The sieved fly ash was washed 2–3 times by distilled water to remove the impurities and preserved in glass bottles. Analytical grade of $\text{ZnSO}_4 \cdot 7\text{H}_2\text{O}$ was used for metal sorption experiments. The stock solution was diluted by serial dilution method as per requirement. The initial pH of the solution was adjusted by using either 0.1 M NaOH or 0.1 M HCl. All the chemicals used for the study were of analytical grade.

Beads preparation

Alginate-fly ash composite beads employed as an adsorbent were prepared in two steps. In the first step, sodium alginate (1 % w/v) in 100 mL distilled water was dissolved followed by addition of known amount of fly ash and agitated for 30 minutes. In the second step the solution of alginate-fly ash was added into a 100 mL solution of 0.1 M CaCl_2 solution drop wise with the help of a syringe with constant stirring. The schematic diagram of bead preparation and the process of turning of sodium alginate into a gel is described in Figure 1.

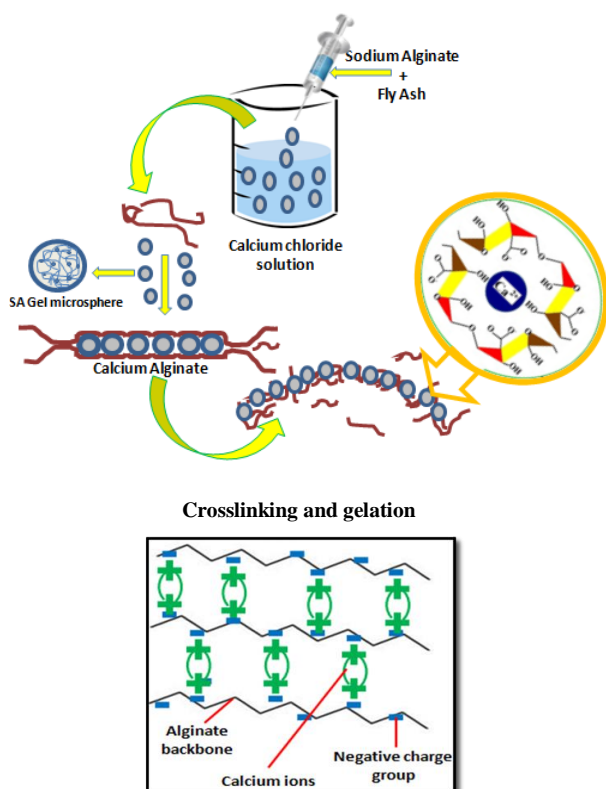


Figure 1. The process of turning a sodium alginate solution into a gel

The produced beads were allowed to harden by leaving them in CaCl_2 solution for 24 h and thereafter filtered and washed thrice with double distilled water. These biopolymeric beads were stored at room temperature in double distilled water and the swollen beads (Figure 2) were used for the adsorption of Zn(II) ions. Immediately before use, the calcium alginate beads were washed again three times with distilled water.

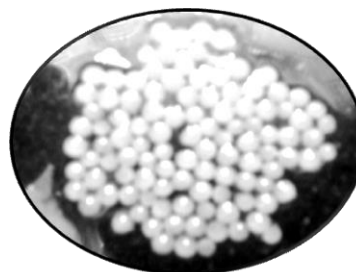


Figure 2. The swollen alginate-fly ash composite beads

FT-IR spectroscopy

FTIR spectra of the composite beads was recorded with an FTIR spectrophotometer (Perkin Elmer, Spectrum BXFTIR Spectrometer) using the KBr (Merck, Germany) disc method.

X-Ray Diffraction (XRD) studies

Powder X-ray diffraction (PXRD) measurements of composite beads was performed on a powder X-ray diffractometer (XPRT PRO Pananalytical, model PW3040160, Netherland) the measurement conditions were Cu K α radiation generated at 40 kV and 30 mA as X-ray source 2– 40° (2θ) and step angle 0.01 ° second⁻¹.

Scanning electron microscopy (SEM) studies

The surface morphology and EDAX analysis of the synthesized beads were examined with the Scanning Electron Microscope (Zeiss EVO 40). A few samples of beads were taken on a copper stub and sputtered with gold for 2 minutes. These gold-coated microspheres were mounted on the SEM instrument and photographs were taken at different magnifications.

Thermal analysis

The thermal stability of the alginate-fly ash composite beads was assessed by the thermogravimetric analyzer. Thermogravimetric analysis was carried out within 30 – 800 °C at 10 °C min⁻¹, in nitrogen flow (TGA 2050 Thermal gravimetric Analyzer).

Beads size

The size of 100 beads was measured by a calibrated scale and their average size was calculated.

Bulk Density

For the determination of bulk density of beads accurately weighed amount of the beads and transferred into 50 mL measuring cylinder. It was subjected to tapping for 3 times and the volume occupied by the beads was noted. Bulk density was estimated by using the following formula.¹⁶

$$\text{Bulk density} = \frac{\text{weight of the beads}}{\text{bulk volume of the beads}}$$

Swelling index

100 mg of dry beads were soaked in pH 7.4 phosphate buffer and the beads were reweighed at regular intervals of time, carefully wiping off the excess liquid with a tissue paper.¹⁷ The under given expression was used for swelling index determination:¹⁸

$$\text{Swelling Index} = \frac{W_t - W_0}{W_0}$$

where

W_t and W_0 are the weight of the beads at time 't' and under dry state, respectively.

Batch adsorption experiments

A stock solution of Zn(II) ions was prepared by dissolving accurate weight of zinc in definite volume of distilled water. Proper concentrations of the adsorbate were prepared from the stock solution through proper dilution. The required concentration for the adsorption experiments were prepared by serial dilution. The initial pH of the solution was adjusted by using either 0.1 M NaOH or 0.1 M HCl. The batch adsorption experiments were performed on an orbital shaker (Khera Lab Instruments). At the end of a predetermined time interval, the adsorbent was removed by filtration and the residual Zn(II) ions was estimated in the filtrate by atomic absorption spectrophotometer (Analytic Jena; ZEE nit 700 P). The effect of initial pH (2–10), agitation time (1–24 h), bead dose (10–80), bead composition (0.1–0.7 g fly ash), and initial metal concentration (5–30 mg L⁻¹) on the adsorption process, as well as to what extent the adsorption data obey Langmuir and Freundlich adsorption isotherms were investigated.

Calculations

The percent removal of metal ions was calculated by using the Eqn. 1.

$$R(\%) = \frac{C_i - C_f}{C_i} \times 100 \quad (1)$$

where,

R is the removal,

C_i is the initial metal concentration and

C_f is the final concentration of the metal ion in mg L⁻¹.

The sorption capacity was calculated from Eqn. 2

$$Q_e = \frac{V(C_i - C_e)}{1000W} \quad (2)$$

where,

Q_e is the adsorption capacity (mg g⁻¹),

C_i is the initial metal concentration (mg L⁻¹),

C_e is the equilibrium concentration of metal (mg L⁻¹),

W is the adsorbent dose (g) and V is the solution volume (mL).

Results and discussion

FTIR Analysis

The infrared spectra for the fly ash (FA), sodium alginate (SA) and composite beads of alginate-fly ash (Alg-F) in the wavelength range of 4000–500 cm⁻¹ is shown in Figure 3.

The IR spectrum of FA, SA and composite beads of Alg-F exhibiting bands at 3435.15 cm⁻¹, 3316.00 cm⁻¹ and 3430 cm⁻¹ which correspond to OH stretching mode in molecular water.¹⁹ In the FTIR spectrum of fly ash, the band at 3435 cm⁻¹ has been assigned to H-O-H stretching vibrations from interlayer water and Si-O-H stretching vibrations of the structural -OH group. The bands at 2924 cm⁻¹ (CH stretching) in FA were also detected.¹⁹ The characteristic band at 1099 cm⁻¹ has been assigned to Si-O stretching vibration. The absorption bands at 797.20 assigned as Si-O vibrations in SiO₂. The absorption bands at 553.84 cm⁻¹ are strong bending vibrations corresponding to Al-O-Si.²⁰⁻²²

In the spectra of SA the characteristic peak of sodium alginate appeared at 820.68 cm⁻¹.²³ The IR spectrum of the pure sodium alginate displayed characteristic peaks at 3316 cm⁻¹, 2944.46 cm⁻¹ and 1610 cm⁻¹ due to O-H, N-H and C=O groups, respectively.²⁴ The adsorption peak of 1610 cm⁻¹ assigned to the asymmetrical stretching vibration of -COO- groups. Small peaks observed at 1610.79-1420.21 cm⁻¹ were attributed to carboxylate groups.²⁵

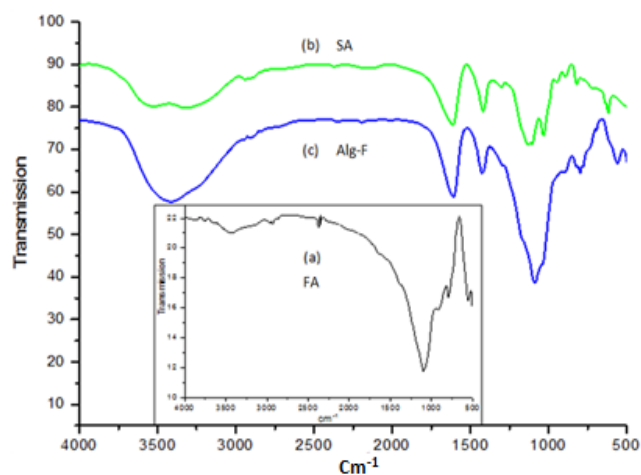


Figure 3. IR Patterns of (a)-Fly ash (FA), (b)- Sodium alginate (SA) (c)- Composite beads, (Alg-F)

In the spectra of Alg-F the characteristic peak of sodium alginate appeared at 819 cm^{-1} was observed. The presence of functional groups of sodium alginate on the surface of beads is verified by peaks at about 3417 cm^{-1} and 2940 cm^{-1} and 1608.06 cm^{-1} due to O-H, N-H and C=O groups, respectively. The peak 3417.97 cm^{-1} has been assigned to the H-O-H stretching vibrations of the interlayer water. The bands at 1608.06 cm^{-1} and 1424.04 cm^{-1} assigned to be bending vibrations of NH and NH_2 and the characteristics peaks of Si-O-Si vibration and SiO_2 was observed at 462.10 cm^{-1} and 798.11 cm^{-1} respectively. However, after the formation of Alg-F beads the absorption peaks in pure sodium alginate at 1026.35 cm^{-1} assigned to the asymmetrical stretching vibration of -COO- groups coupled with the peaks at 1032.22 cm^{-1} and shifted to 1688.08 cm^{-1} . The absorption bands at 560.53 cm^{-1} are strong bending vibrations corresponding to Al-O-Si. The presence of these bands in Alg-F complex indicates the presence of fly ash in the alginate matrix but the intensity of this peak is increased compared to fly ash and sodium alginate. Furthermore, the bands at about 3441.80 cm^{-1} and 3316 cm^{-1} , which were the stretching vibration of groups involved in both inter and intramolecular hydrogen bonds, broadened and coupled with -OH band of sodium alginate at 3400 cm^{-1} , induced by the addition of sodium alginate to fly ash implying that the occurrence of hydrogen bonds between -OH groups of sodium alginate and fly ash molecules. Small peaks observed at $1614.98\text{--}1423.42\text{ cm}^{-1}$ were attributed to carboxylate groups.²⁵

All the spectra show presence of several -OH and -COOH groups. Hydrogen of these groups is capable of ion exchange with metal cation.

XRD Analysis

The XRD patterns of fly ash (FA), composite beads before adsorption (Alg-F) and after adsorption (Alg-FM) are shown in Figure 4. Sodium alginate is usually crystalline due to strong interaction between the alginate chains through intermolecular hydrogen bonding.²⁶

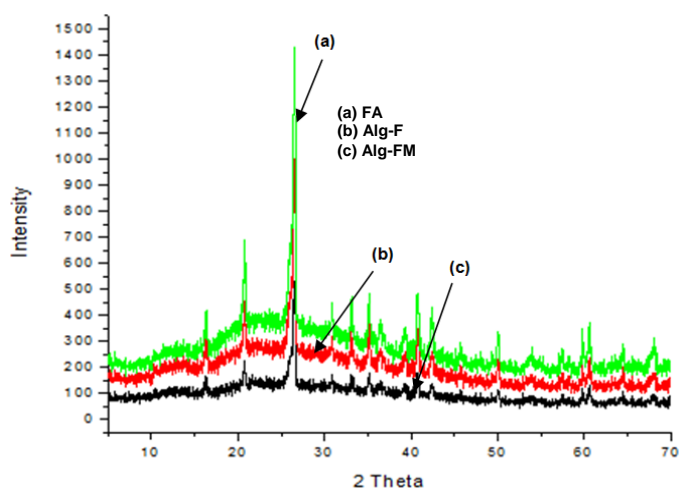


Figure 4. XRD Patterns of (a)-Fly ash (FA), (b)- Alginate-fly ash composite beads (Alg-F), (c)-Composite beads after metal adsorption, (Alg-FM)

It was observed that the fly ash consisted of crystalline minerals mullite, quartz, hematite and small amounts of calcium oxide with large characteristic peaks of quartz (SiO_2). This result is similar to that reported for a fly ash investigated.²⁷ It can be observed that there are no significant differences for all XRD profiles but the large characteristic peaks of quartz (SiO_2) in the Alg-F than those for Alg-F and Alg-FM are indicative of large SiO_2 concentrations. The intensity of quartz is very strong, with mullite forming a chemically stable and dense layer. The FA is of lower activity and at this state its glassy surface layer particles is dense, chemically stable and also protected the more active inner constituents of the fly ash comprises of porous, spongy and amorphous particles. Three diffraction peaks at 2θ values 16° , 21° and 41° were observed for sodium alginate.

In case of Alg-F, the intensity of diffraction peaks of alginate decreased notably which indicates that the nucleation and growth of semiconductor or metal particles affected the crystalline nature of sodium alginate. The pattern of fly ash has sharp peaks showing the crystalline nature of the fly ash. After the formulation of beads the XRD patterns shows very weak, unoriented, hump like shape indicating Alg-F is an amorphous material.²⁸

The low degree of crystallinity shows that *in-situ* nucleation leads to the formation of very small nuclei and interaction with the polymer prevent any further crystallization of fly ash. If sodium alginate and fly ash have low compatibility, each polymer would have its own crystal region, so X-ray diffraction patterns are expressed as simply mixed patterns of sodium alginate and fly ash with the same ratio. However, in comparison to fly ash the patterns of the Alg-F show that the intensity of diffraction peak between 2θ values $12^\circ\text{--}36^\circ$ decreased. This means intermolecular hydrogen bonds between sodium alginate and fly ash and was introduced, which destroyed the original molecular structure of sodium alginate, resulting in the changes of diffraction patterns.

Same pattern was observed after the adsorption of metal on alginate-fly ash beads (Alg-FM), the XRD patterns of the shows decrease in the intensity of diffraction peaks than Alg-F. This means intermolecular hydrogen bonds between Alg-F and metal were introduced, which destroyed the original molecular structure of Alg-F, resulting in the changes of diffraction patterns.

SEM Studies

SEM images of Alginate-fly ash (Alg-F) beads taken at different magnification are shown in Figure 5. The beads are found to be around $100\ \mu\text{m}$ and the SEM images reveal the presence of pores on the surface and the beads were almost spherical in shape with networked and smooth surfaces. The SEM of the microbeads prepared with sodium alginate are spherical in shape exhibits a sandy appearance. The image portrays layers of crosslinked polymers that are formed inside the bead. At magnification 1.1 KX bridging and dense nature of beads is due to coalescence and fusion to the colloidal aqueous polymer dispersions in the alginate-fly ash matrix.

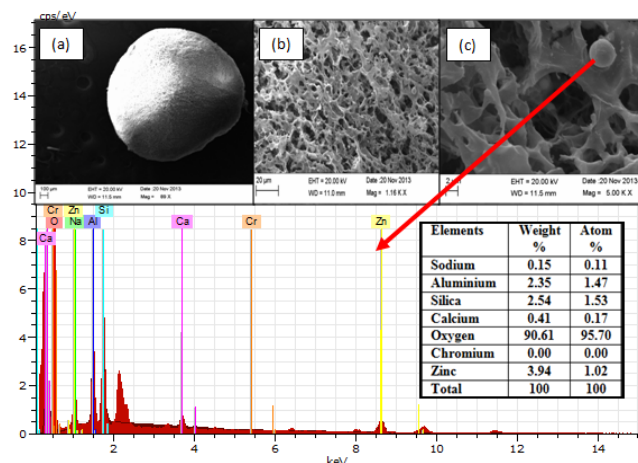


Figure 5. Scanning electron micrographs and EDAX of alginate-fly ash beads

The EDAX analysis of the bead surface disclosed the beads composition. EDAX is the microanalysis technique that could provide information of the bulk composition.²⁹ Evidently, EDAX peaks of metals and each element used for the synthesis along with notable amount of oxygen from alginate backbone on the surface of the beads.

Thermal Studies

The TGA/DTA thermogram of alginate-fly ash beads (Alg-F) shows (Figure 6) high thermal stability in the temperature region of 30-900 °C. The Alg-F shows three zones of weight loss. TGA shows the onset of decomposition near 30 °C which is due to the loss of water molecules trapped in the samples.

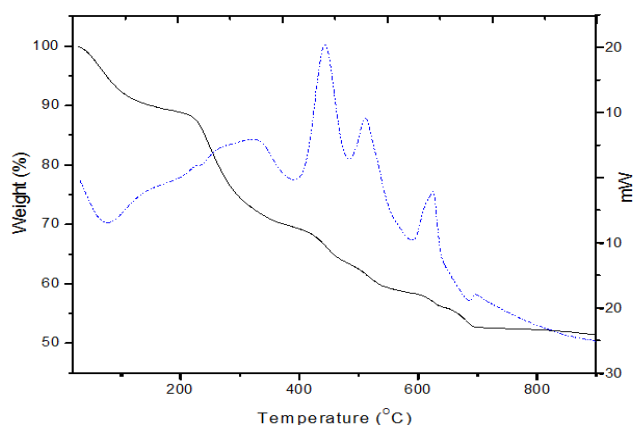


Figure 6. The TGA/DTA thermogram of alginate-fly ash beads (Alg-F)

DTA curves shows an endothermic peak at 75.85 °C attributed to the loss of water absorbed in the beads, the exothermic peak at 442.12, 513.02 and 625.77 °C means the taking place of thermal degradation of intermolecular side chain. Second weight loss was observed in the temperature range from 29-214 °C, implying that the occurrence of different extent thermal degradation of sodium alginate, rupture of alginate chains. Third weight loss was observed approximately 35 % from 409-902 °C indicates the rupture of chains, fragments, and monomers

resulting in 51 % residual. Weight loss in the temperature range from 600-750 °C is due to the loss of hydroxyl groups in the aluminosilicate structure. Significant changes of DTA curves of the beads suggest that a strong interaction established between sodium alginate and fly ash molecules.

TGA curve of beads after metal adsorption (Alg-FM) shows three thermal decomposition stages (Figure 7). The first weight loss of 12 % from 32-200 °C corresponds to the evaporation of free water. DTA curves show an endothermic peak at 68.63 °C due to the loss of water bound to the cations present within the interlayer.

Second weight loss of 60 % was observed 200-286 °C indicates which resulted from the greatest thermal degradation of the thermal degradation of sodium alginate along with decomposition of metal adsorbed on beads.

DTA curves shows a sharp exothermic peak at 247.06 °C which resulted from the greatest thermal degradation of the zinc. Third major weight loss was observed approximately 60% from 300-700 °C indicates the rupture of chains, fragments, and monomers resulting in 19% residual.

The starting temperature of the greatest thermal degradation increased in the sequence of Alg-F (214.78) > Alg-FM (188.60 °C), which is the same as that of their crystallinity, implying thermal stability of the beads were improved by their crystalline domains and hydrogen bonding interactions.³⁰

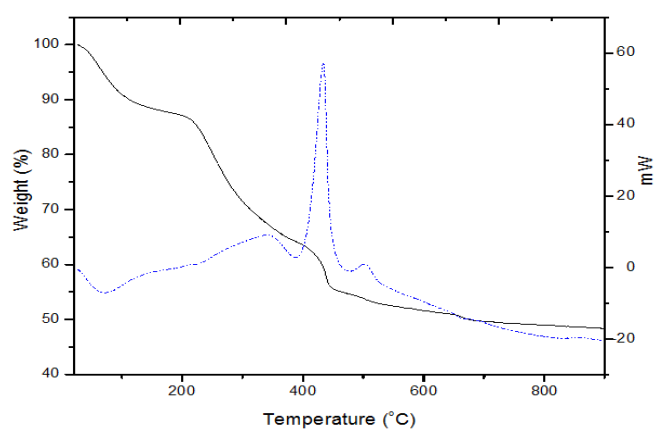


Figure 7. The TGA/DTA thermogram of alginate-fly ash beads after metal adsorption (Alg-FM)

Apart from this the average size, bulk density and swelling ratio of beads calculated are; 0.12 cm, 0.34 g mL⁻¹ and 28.65 respectively.

Batch Adsorption Studies

Effect of pH

The adsorptive behavior of Zn(II) ions was studied from the aqueous solution at different pH values are the principle factor influencing the adsorptive capacities of Zn(II) ions on alginate-fly ash beads. The pH of the aqueous solution is an important controlling parameter in the adsorption process. As the solution pH increase, the onset of the metal hydrolysis and precipitation began at pH >7 and the onset of

adsorption therefore occurs before the beginning of hydrolysis.³¹ When the pH of the adsorbing medium was increased from 2-6, there was a corresponding increase in de-protonation of the adsorbent surface, leading to decrease in H^+ ion on the adsorbent surface, which favours adsorption of positively charge species and the positive sites on the adsorbent surface.^{32,33} The results obtained are shown in Figure 8, which shows the effect of pH on the adsorption of Zn(II) ions from the aqueous solution on fly ash composite beads.

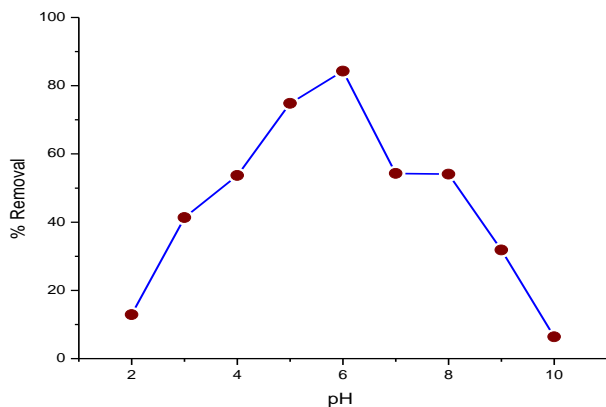


Figure 8. Effect of pH on removal of Zn(II) ions

It is clear that Zn(II) ions was effectively adsorbed in the pH range of 4-6 and the maximum adsorption of ion fly ash beads occurred at pH 6 thus, pH 6 is chosen for all experiments. The decrease in adsorption at pH greater than 6 is probably due to the formation of hydroxide. This is in agreements with the results obtained by Khalid *et al.*³⁴ for adsorption of lead on rice husk. The hydrolysis of cations occurs by the replacement of metal ligands in the inner coordination sphere with the hydroxyl groups.³⁵ This replacement occurs after the removal of the outer hydration sphere of metal cations. Adsorption may not be related directly to the hydrolysis of the metal ion, but instead of the outer hydration sphere that precede hydrolysis.

Most probably, the removal of Zn(II) ions from the aqueous solution by alginate-fly ash beads involves a complex mechanism which is partly controlled by adsorption and partly by the chemical precipitation at the solid solution interface and also partly by the pore filling mechanism.³⁶

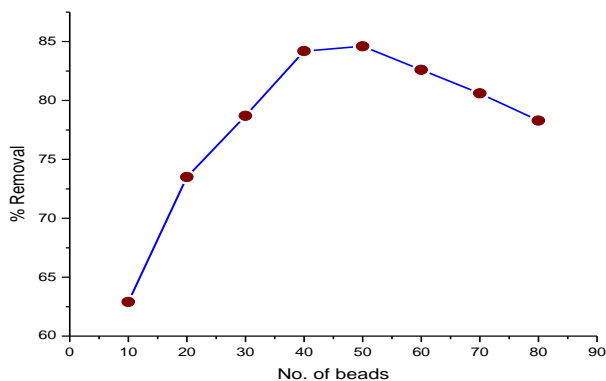


Figure 9. Effect of beads dose on removal of Zn(II) ions

Effect of adsorbent dose

The effect of adsorbent dose on the adsorption of these metal ions by varying amount of bead dose is shown in Figure 9. It was observed that the dose of beads (10–80) definitely influences the amount of adsorbed metal ions. It was observed that percentage removal of zinc was increased with the increase of no. of beads up to 40 beads. Further, the increase in beads reduces the percentage removal of Zn(II) ions to some extent.

The adsorption of metal ions on alginate-fly ash beads may involve metal interaction.³⁷ and co-ordination to functional. According to Shukla *et al.*,³⁸ the decrease in adsorption with increase in adsorbent dose is due to the high number of unsaturated sites.

Effect of bead composition

The effect of fly ash composition in the beads on the adsorption of the Zn(II) ions is shown in Figure 10. It was observed that the amount of adsorbent dose in the range (0.1–0.7 g) definitely influences the amount of adsorbed metal ions.

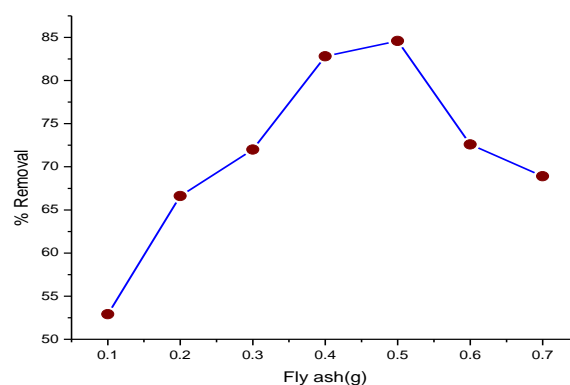


Figure 10. Effect of bead composition on removal of Zn(II) ions

It was observed that percentage removal increased with the increasing the concentration of fly ash up to 0.5 g, where it was maximum. Further, the increase in fly ash amount in the beads composition reduces the percentage removal of Zn(II) ions due to high number of unsaturated sites.³⁸

Effect of contact time

The effect of contact time on the adsorption of Zn(II) ions is shown in Figure 11. The results indicated that increase in the contact time increased the metal uptake but remained constant after an equilibrium time.

The uptake of Zn(II) ions was rapid and the equilibrium was attained in 8 hours of contact between the adsorbent and metal solution. According to Bhattacharya and Gupta³⁹ the initial high rate of metal uptake may be attributed to the existence of the base surface. However, the number of available adsorption sites decreased as the number of metal ions adsorbed increases.

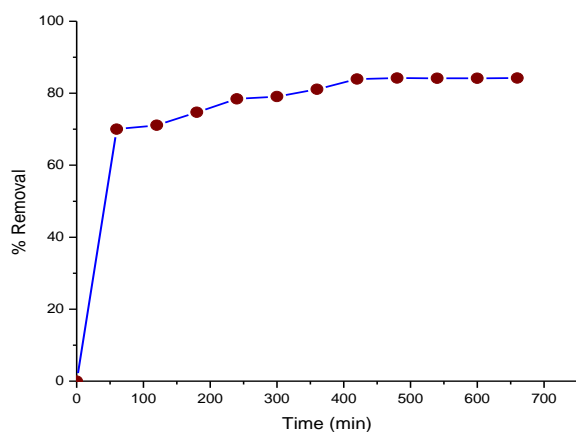


Figure 11. Effect of contact time on removal of Zn(II) ions

The enhanced adsorption of metal ions with in agitation time may also in boundary resistance to mass transfer in the bulk solution and an increase in the kinetic energy of hydrated ion.⁴⁰ By increasing the agitation time, the boundary layer resistance will be reduced and there will be an increase in the mobility of ions in the solution.

Adsorption models

Since, the adsorption isotherm is important to describe how adsorbate will interact with adsorbents and so is critical for design purpose, therefore, data using an equation is essential adsorption operation.⁴¹ Modelling of equilibrium data is fundamental for the industrial application of adsorption since it gives information for comparison among different adsorbent under different operational conditions, designing and optimizing operation procedure.⁴²

The result of batch equilibrium was used to characterize the equilibrium between the amount of adsorbate that accumulated on the adsorbate and the concentration of dissolve adsorbate. The experimental isotherm data set obtained was fitted using adsorption models including the Langmuir and Freundlich isotherm.^{43, 44}

The isotherm constants of Langmuir and Freundlich were calculated using normal linearization method.

Freundlich model

The adsorption data have been fitted to the Freundlich isotherm. Its linearised form is represented by Eqn. 3.

$$\lg Q_e = \lg K + \frac{1}{n} \lg C_e \quad (3)$$

where,

C_e is the equilibrium concentration (mg L^{-1}),

Q_e is the amount adsorbed (mg g^{-1})

K is adsorption capacity and

$1/n$ is adsorption intensity.

A plot of $\log Q_e$ versus $\log C_e$ gives a straight line of slope $1/n$ and intercept K is shown in Figure 12.

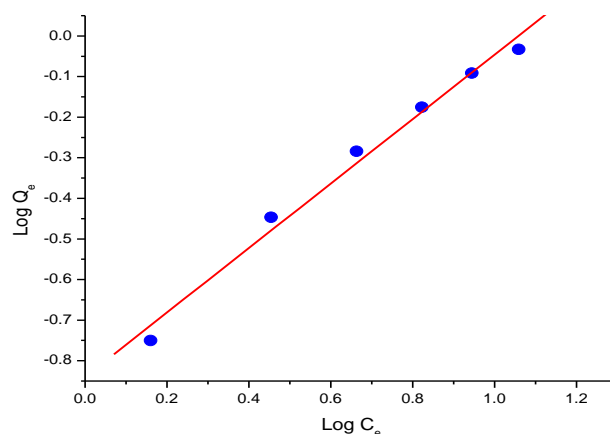


Figure 12. The linearized plot for the Freundlich adsorption isotherm of Zn(II) ions using biopolymer composite beads of alginate-fly ash

Langmuir model

The capacity of metal binding was determined by plotting C_e/Q_e against C_e , using the Langmuir equation. The plot of the specific sorption C_e/Q_e against equilibrium concentration C_e gave the linear isotherm parameters Q_{\max} , b and the coefficient of determination (R^2). The linear equation of Langmuir represented as Eqn. - 4.

$$\frac{C_e}{Q_e} = \frac{1}{Q_{\max} b} + \frac{C_e}{Q_{\max}} \quad (4)$$

where,

C_e is the metal concentration in the solution at equilibrium (mg L^{-1}),

Q_{\max} (adsorption capacity) and

b (energy of adsorption) are the Langmuir constants.

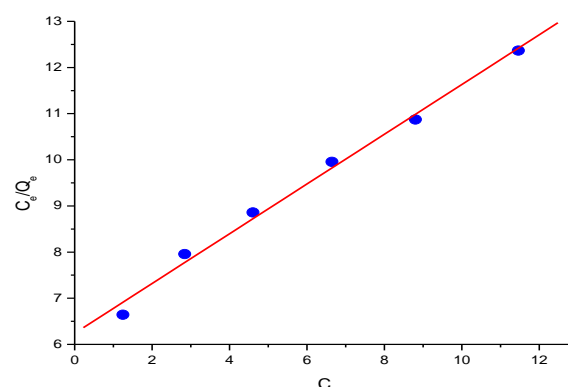


Figure 13. The linearized plot for the Langmuir adsorption isotherm of Zn(II) ions using biopolymer composite beads of alginate-fly ash

The Langmuir isotherm model effectively describes the sorption with R^2 values. The sorption capacity, Q_{\max} which is a measure of maximum adsorption capacity corresponding to complete monolayer coverage showed that composite beads of alginate-fly ash beads had a mass capacity for Zn(II) ions is 1.8554 mg g^{-1} .

The adsorption coefficient b which is related to the apparent energy of adsorption Zn(II) ions is 0.0860. The plots of C_e/Q_e against C_e for adsorption of Zn(II) ions gave a straight line are shown in Figure 13. It has seen that the linear fit is fairly good and enables the applicability of the Langmuir model to the Zn(II) ions adsorption on the alginate-fly ash composite beads.

The essential characteristics of Langmuir equation can be described by dimensionless equilibrium parameter,⁴⁵ R_L which is defined as;

$$R_L = \frac{1}{1 + bC_0} \quad (5)$$

where,

b is the Langmuir constant

C_0 is the initial metal concentration of Zn(II) ions.

In the present study the R_L for Zn(II) ions were found between 0 and 1 as shown in Figure 14, for the initial concentration of Zn(II) ions of 5-30 mg L⁻¹ indicating that the adsorption of Zn(II) ions is favorable. The R_L values indicate the shape of isotherm as shown in Table 1. The R_L values between 0 and 1 indicate favorable adsorption.⁴⁶

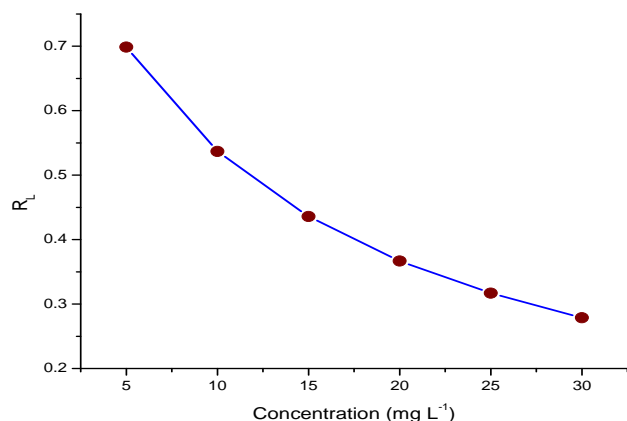


Figure 14. R_L vs initial concentration of metal ions

Table 1. Relationship between R_L and type of isotherm

| R_L | Type of isotherm |
|-----------|------------------|
| $R_L > 1$ | Unfavourable |
| $R_L = 1$ | Linear |
| $R_L < 1$ | Favourable |
| $R_L = 0$ | Irreversible |

Examination of correlation coefficient suggests that both the isotherms models fitted well for the sorption of Zn(II) ions. This isotherm does not predict any saturation of the sorbent by the sorbate; thus infinite surface coverage is predicted mathematically, indicating multilayer adsorption on the surface.⁴⁷ The correlation coefficient of data for Langmuir and Freundlich plot give a value which is > 0.9 although this value for Freundlich isotherm is slightly higher

than that of Langmuir isotherm since, the correlation coefficient for both are high, it reveals that besides monolayer adsorption there is multilayered adsorption and also suggests that adsorption reaction is physico-chemical type.

The values of both Langmuir and Freundlich isotherm parameters were given in Table 2. Examination of data suggests that Freundlich isotherm is a good model for the sorption of Zn(II) ions. The values of $1/n$ that vary between 0.1 and 1.0 indicate the favorable adsorption of heavy metals.⁴⁸

Table 2. Langmuir and Freundlich adsorption parameters for the adsorption of Zn(II) ions at 30 °C.

| Langmuir Parameters | | Freundlich Parameters | |
|-----------------------------------|--------|-----------------------|--------|
| Q_{max} , (mg g ⁻¹) | 1.8554 | K | 1.2610 |
| b (L, mg ⁻¹) | 0.0860 | $1/n$ | 0.1449 |
| R^2 | 0.9700 | R^2 | 0.9860 |

The Langmuir model deals with monolayer coverage and constant adsorption energy while Freundlich equation deals with physicochemical adsorption on heterogeneous surfaces.⁴⁹ The applicability of both these isotherms to the alginate-fly ash composite beads, in the present study, implies that monolayer adsorption and heterogeneous surfaces conditions exist under the experimental conditions used. The adsorption properties of the adsorbent are thus likely to be complex, involve more than one mechanism.

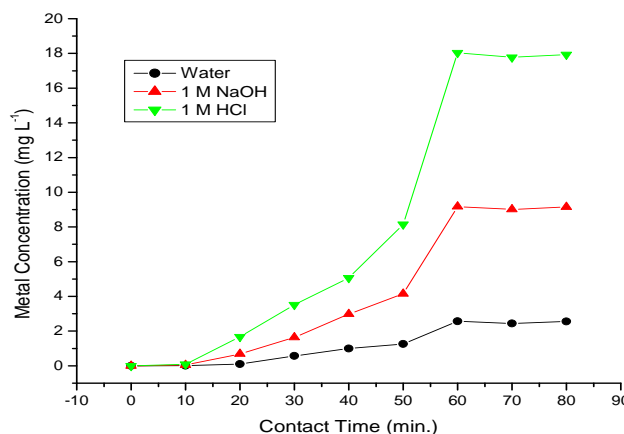


Figure 15. Desorption profile for Zn(II) ions

Desorption studies

In order to desorb the metal ions, the beads loaded with Zn(II) ions were exposed to 20 mL of distilled water, 0.1 M HCl and 0.1 M NaOH separately for 15 minutes and washed with double distilled water. It was found that 0.1 M HCl is the better eluent for desorption of metal from the beads (Figure 15). The beads were then again exposed to distilled water, followed by 0.1 M HCl, to strip any remaining Zn(II) ions. The desorbed beads were reused in next adsorption experiments. In order to show the multiple reuse of adsorbent beads, an adsorption-desorption cycle of metal ions was repeated three times using the same preparations.

Conclusions

This work indicates that alginate-flyash composite beads can be used for removal of Zn(II) ions from wastewater. Both Langmuir and Freundlich isotherm models can be used to estimate maximum metals uptake and the affinity parameter. It was found that the adsorption equilibrium data was better fitted by both the Freundlich and the Langmuir isotherm in the concentration range studied. The removal of Zn(II) ions was found to depend on adsorbent dosage, composition of beads, solution pH and contact time. Solution pH is an important parameter affecting adsorption of ions and maximum removal for Zn(II) ions at pH value 6.0. The adsorption mechanism of Zn(II) ions on alginate-fly ash composite beads involves either cation exchange or complexation between the metal cation and the hydroxide ion in the solution. This study shows a new trend for using alginate-fly ash composite beads for the benefit of environmental pollution control.

Acknowledgements

Authors are thankful to the Head, Department of Chemistry, Director, USIC, University of Delhi, and Director of AIRF-Jawaharlal Nehru University for providing instrumentation facilities and UGC [F.15-76/12 (SA-II)] for providing financial assistance.

References

- ¹Ayoub, G. M., Semerjian, L., Acra, A., El Fadel, M. and Koopman, B., *J. Env. Eng.*, **2001**, 27, 196-207.
- ²Ho, Y. S. M., *Water Res.*, **2003**, 37, 2323-2330.
- ³Inbaraj, B. S., Selvarani, K. and Sulochana, N., *J. Sci. & Ind. Res.*, **2002**, 61, 971-978.
- ⁴Lo, W. H., Chua, H., Lam, K. H. and Bi, S. P., *Chemosphere*, **1999**, 39, 2723-2736.
- ⁵Mellah, A. and Chegrouche, S., *Water Res.*, **1997**, 31, 621-629.
- ⁶Undaybeytia, T., Morillo, E. and Maqueda, C., *Clays Clay Min.*, 1996, 31, 485-490.
- ⁷Mangale Sapana, M., Chonde Sonal G. and Raut, P. D., *Res. J. Recent Sci.*, **2012**, 1(3), 31-40.
- ⁸Vaishnav, V., Kailash, D., Suresh C. and Madan, L., *Res. J. Recent Sci*, **2012**, 1, 160-165.
- ⁹Bilodeau, A. and Malhotra, V. M., *ACI Mater. J.*, **2000**, 97, 4-49.
- ¹⁰Ahmaruzzaman, M., *Adv. Colloid Interface Sci.*, **2008**, 143, 48-67.
- ¹¹Wang, S. and Wu, H., *J. Hazard. Mater.* **2006**, 136, 482-501.
- ¹²Wang, S. B., Soudi, M., Li, L. And Zhu, Z. H., *J. Hazard. Mater.*, **2006**, 133, 243-251.
- ¹³Aravindhnan, R., Fathima, N. N., Rao, J. R. and Nair, B. U., *Colloids and Surfaces A: Physicochemical and Engineering Aspects*, **2007**, 299, 232-238.
- ¹⁴Davis, T. A., Volesky B. and Mucci, A., *Water Research*, **2003**, 37, 4311-4330.
- ¹⁵Kuyucak, N., and Volesky, B., *Biotechnol. Bioeng.*, **1989**, 33, 823-831.
- ¹⁶Ashok Kumar, A., Rajesh Kumar, P., Anil Kumar, A., Lokeswara Reddy, K., Murthy, T. E. G. K. and Venkateswara Rao, T., *Journal of Applied Pharmaceutical Science*, **2011**, 01 (06), 127-132.
- ¹⁷Kanaka Durga Devi, N., Chandana, M., Sindhura, A., Ratnavali, G. and Kavitha, R., *Pharmacophore*, **2010**, 1(3), 196-213.
- ¹⁸Sonone, S. B., Kokane, S. P., Shirote, P. J. And Naikawade, N. S., *Inter. Jour. of Pharm. Tech. Res.*, **2011**, 3(1), 225-230.
- ¹⁹Freddi, G., Tsukada, M. and Beretta, S., *J. Appl. Polym. Sci.*, **1999**, 71, 1563-1571.
- ²⁰Meng, M., Zhou, N. L., Zhang, S, Q. and Shen, J., *Int. J. Pharm.*, **2009**, 382, 45-49.
- ²¹Joshi, G. V., Patel, H. A., Bajaj, H. C. and Jasra, R. V., *Colloid. Polym. Sci.*, **2009**, 287, 1071-1076.
- ²²Chen, B. Y., Lee, Y. H., Lin, W. C., Lin, F. H. and Lin, K. F., *Biomed. Eng. Appl. Basis Commun.*, **2006**, 18(1), 30-36.
- ²³Zhang, L., Zhou, D., Wang, H., and Sheng, S., *J. Membrane Sci.*, **1997**, 124, 195-201.
- ²⁴Nikolic, C. V., Nikolic, L. J., Stankovic, M., Kapor, A., Popsavin, M. and Cvetkovic, D., *J. Serb. Chem. Soc.*, **2007**, 72, 737-746.
- ²⁵Stuart, B., *Modern Infrared Spectroscopy*, Wiley, Chister, U.K., **1996**.
- ²⁶Fang, D., Liu, Y., Jiang, S., Nie, J. and Ma, G., *Carbohydr. Polym.*, **2011**, 85, 276-279.
- ²⁷Sarkar, A., Bassu, A. K., Udaybhanu, G. and Rano, R., *Fuel*, **2006**, 87, 259-277.
- ²⁸Yan, F., Zheng, C. R., Zhai, X. D. and Zhao, D. J., *J. Appl. Polym. Sci.*, **1998**, 67, 747-754.
- ²⁹Velásquez, P., Leinen, D., Pascual, J., Ramos-Barradoa, J. R., Cordova, R. and Gómez, H., *J Electroanal Chem.*, **2001**, 510, 20-28.
- ³⁰Liang, C. X. and Hirabayashi, K., *J. Appl. Polym. Sci.*, **1992**, 45, 1937-1943.
- ³¹Baes, G. B. and Mesmer, R. E., "Hydrolysis of Cations", John Wiley and Sons, New York, **1976**.
- ³²Kadirvelu, K. and Namasivayam, C., *Adv. Environ. Res.*, **2003**, 7, 471-478.
- ³³Abdus-Salam, N. and Adekola, F. A., *Afr. J. Sci. Technol.*, **2005**, 6, 55-66.
- ³⁴Khalid, N., Ahmad, S., Naseer Kiani, S. and Ahmed, J., *Sep. Sci. Technol.*, **1998**, 33, 2349-2362.
- ³⁵Badmus, M. A. O., Audu, T. O. K. and Anyata, B. U., *Turkish J. Eng. Env. Sci.*, **2007**, 31, 251 - 263.
- ³⁶Knocke, W. R. and Hemphill, L. M., *Water Res.*, **1981**, 15, 275-282.
- ³⁷Sengupta, A. K. and Clofford, D., *Environ. Sci. Technol.*, **1986**, 20, 149-155.
- ³⁸Shukla, A., Zhang, Y. H., Dubey, P., Margrave, J. L. and Shukla, S. S., *J. Hazar. Mater*, **2002**, B95, 137-152.
- ³⁹Bhattacharya, K. G. and Gupta, S. S., *Colloid Surf. A: Physiochem. Eng. Asp.*, **2006**, 277, 191-200.
- ⁴⁰Horsfall, M. and Abia, A. A., *Water Res.*, **2003**, 37, 4913-4923.
- ⁴¹Hashem, M. A., Abdelmonem, R. M. and Farrag, T. E., *Alexandria Eng. J.*, **2007**, 1, 1-9.
- ⁴²Benguella, B. and Benaissa, H., *Water Res.*, **2002**, 36, 2463-2474.
- ⁴³Langmuir, I., *J. Am. Chem. Soc.*, **1918**, 40, 1361-1402.
- ⁴⁴Freundlich, H., *Z. Phys. Chem.*, **1907**, 57, 385-470.

⁴⁵Hall, K. R., Eagleton, I. C., Acrivos, A. and Vermeulen, T., *Ind. Eng. Chem. Fund.*, **1966**, 5, 212-223.

⁴⁶Ahalya, N., Kanamadi, R. D. and Ramachandra, T. V., *Indian J. Chem. Technol.*, **2006**, 13, 122-127.

⁴⁷Hasany, S.M., Saeed, M. M. and Ahmed, M., *J. Radioanal. Nucl. Chem.*, **2002**, 252, 477-484.

⁴⁸Unnithan, M. R. and Anirudhan, T. S., *Indian Eng. Chem. Res.*, **2001**, 40, 2693-2701.

⁴⁹Singh, K. K., Singh, A. K. and Hasan, S. H., *Bioresour. Technol.*, **2006**, 97, 994-1001.

Received: 31.03.2014.

Accepted: 28.05.2014.